HMS Aerogel Cerenkov Calibration for Fpi-2

Garth Huber (huberg@uregina.ca)
February 26, 2004

Abstract

Details regarding the calibration of the HMS aerogel Cerenkov detector are presented.

1 Calibration Method

The aerogel Cerenkov adcs were calibrated with a new kumac titled `haero_calib.kumac`. The main points of this calibration are as follows:

1. The calibration kumac makes use of the haero-npe-pmt histograms rather than the typically-used raw adc spectra. This is because the haero-npe-pmt histograms have had their pedestals subtracted, where the pedestals are determined from the 1000 pulser events at the start of every run. As shown in this report, this treatment of the pedestal yields a stable calibration, and so seems to be an appropriate way to proceed.

2. Because the pedestals are already subtracted, in order to calibrate the detector it is only necessary to determine the pmt gain parameters. These correspond to the adc values of the single photoelectron peaks, after pedestal subtraction.

3. As shown in Fig. 1, the 1 p.e. peak positions are determined by fitting a Gaussian to the top of the 1 p.e. peak. The region of channels for which the fit is determined is very restricted, in order to keep the fit value from being skewed by the non-Gaussian shape of the rest of the histogram.

4. A caution to future users of this kumac is that because of the use of the haero-npe-pmt histograms, the initial gain parameters stored in `haero.param`, used in the first replay of the data, must be consistent with those assumed in the `haero_calib.kumac`, so that the correct gain parameters can then be calculated from the haero-npe-pmt data. If these two sets of parameters are inconsistent, erroneous gain parameters will be output.

This method differs from the earlier calibration algorithm used by the Yerevan group `h_aero_calib.kumac` in several important ways.

1. The raw adc spectra are used, after being passed through a smoothing procedure.

2. The maximum count channels in the region of the pedestal and the region of the 1 p.e. peak are used, rather than the pulser value and Gaussian fit value, respectively. The gain parameter is then calculated from the difference of the two maximum count channels.

The results of the two calibration methods can be directly compared.

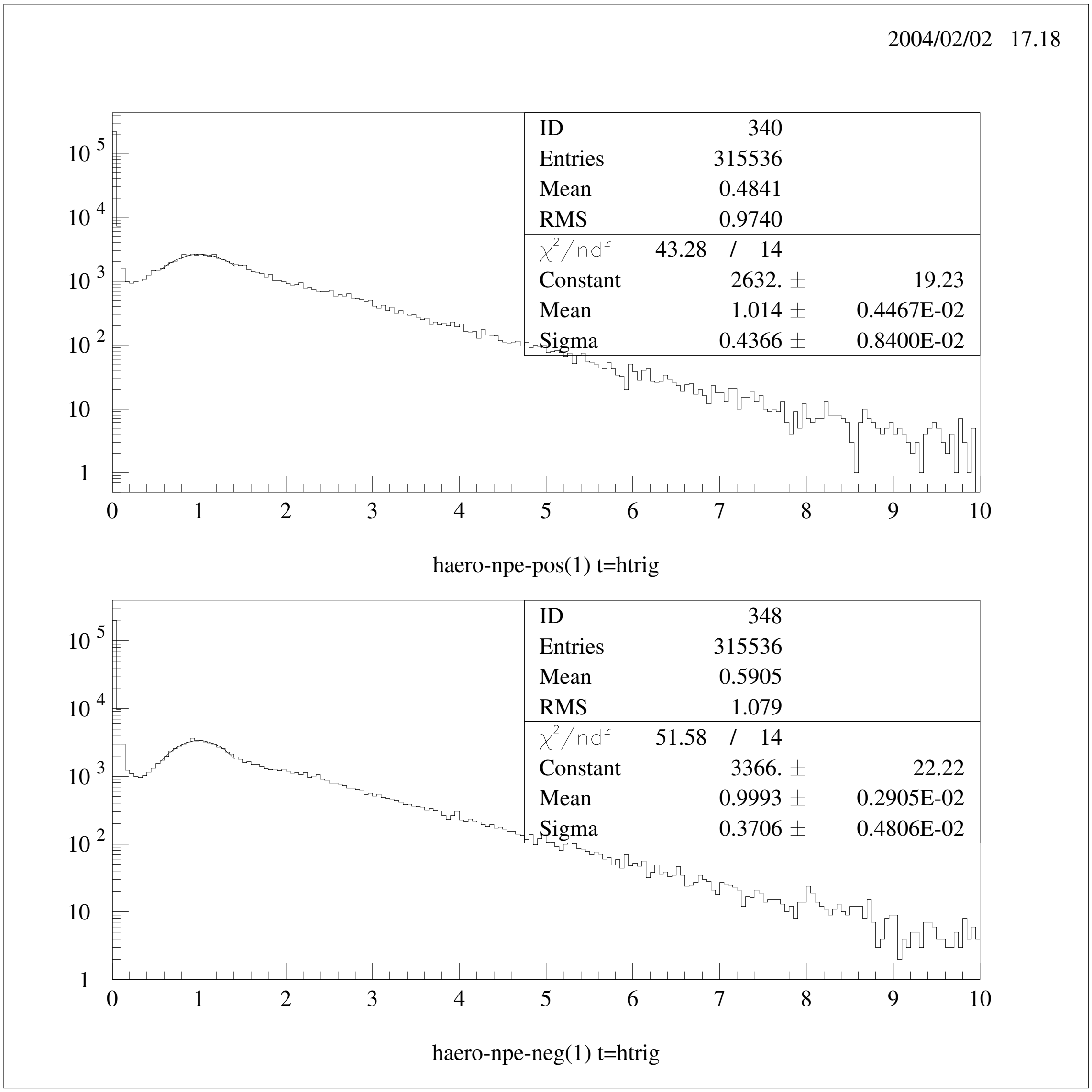

Figure 1: Example histogram fits from run 47182. You must look very carefully in the region from 0.7 to 1.3 p.e. to see the Gaussian fit. Here, the means of the fitted Gaussians are very close to 1.0, which indicates that the photoelectron calibration for this run is already quite good.

2 Calibration Run Dependence

Calibration parameters for all 16 pmts and for 42 Fpi-2 runs are shown in Figs. 2 and 3. As the adcs (after pedestal subtraction) are divided by the plotted number to obtain the number of photoelectrons, larger numbers correspond to higher pmt gain. Each plot covers the full 5 week running period of the experiment, and only includes runs which are appropriate for calibration (i.e. high rate tests, low statistics runs, or those dominated by protons, are excluded).

It is immediately apparent that using either calibration method, all 16 pmts exhibit similar slow increases in gain with time. It is also clear that the scatter in the gain parameters obtained with the 'Huber' kumac is much less than that obtained with the old 'Tadevosyan' kumac. It was decided to use the 'Huber' kumac results for all further studies, because of their greater consistency.

The long-term gain increase of each pmt is possibly due to an undetermined temperature co-efficient of the amplified bases used. Another possibility is that this is due to the bake-out period of the new PMTs, during which their performance slowly improves, but this seems unlikely, given the multi-week time scale of the plot.

There are also short-term gain changes, of the order of a few percent, which are correlated among many of the pmts. These shifts may be due to changes in stray magnetic fields when the HMS settings are altered. An extensive set of parameter files have been made, in order to track these short-term gain changes. All necessary files have been placed in the CVS repository.

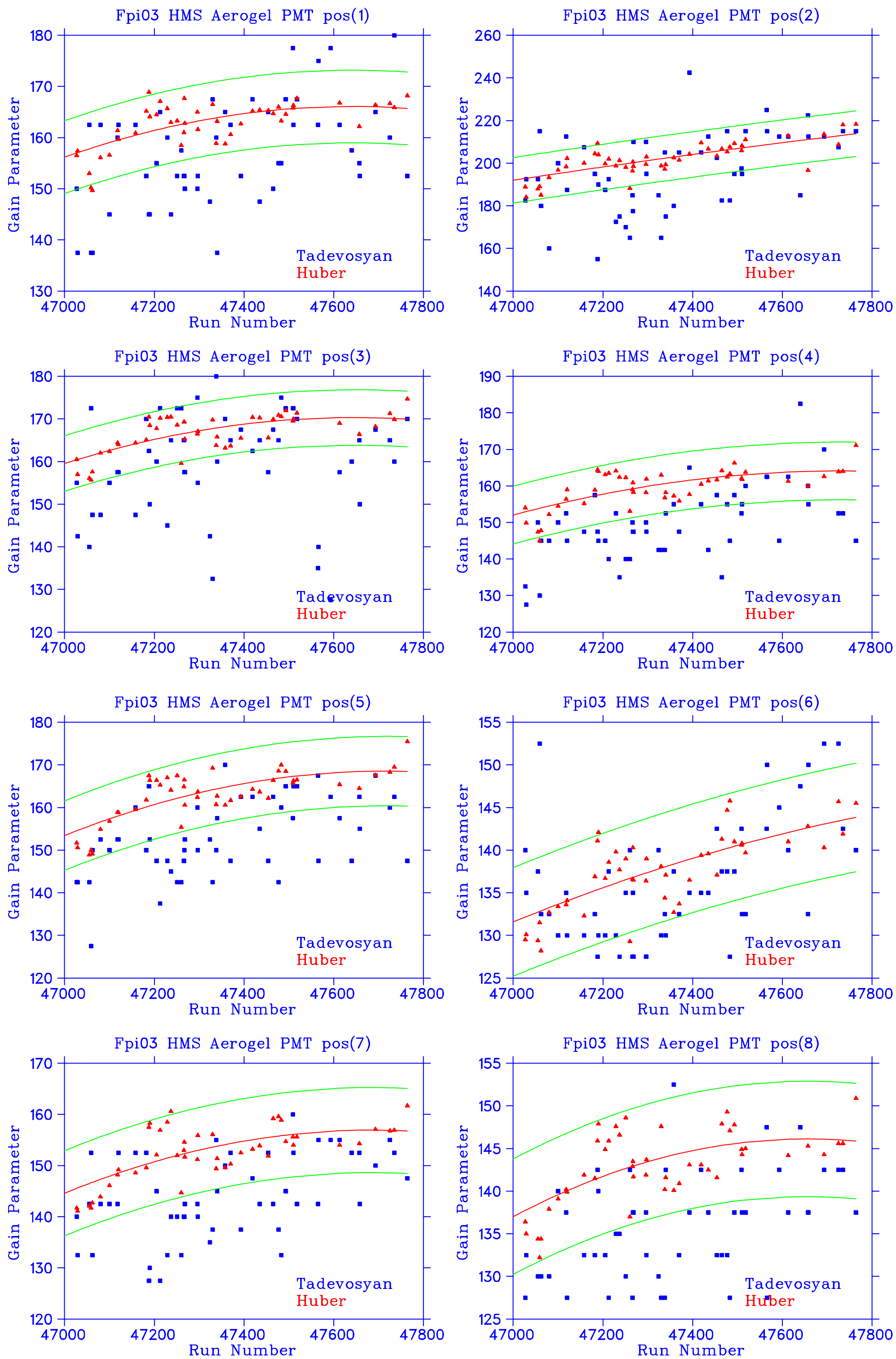

Figure 2: Gain parameters for positive pmts 1-8. It is clear that the 'Huber' calibration routine produces a more consistent set of gain parameters than the early 'Tadevosyan' method. In addition, the early Yerevan method under-estimates the gain parameter value, resulting in a small over-estimate of the number of detected photoelectrons.

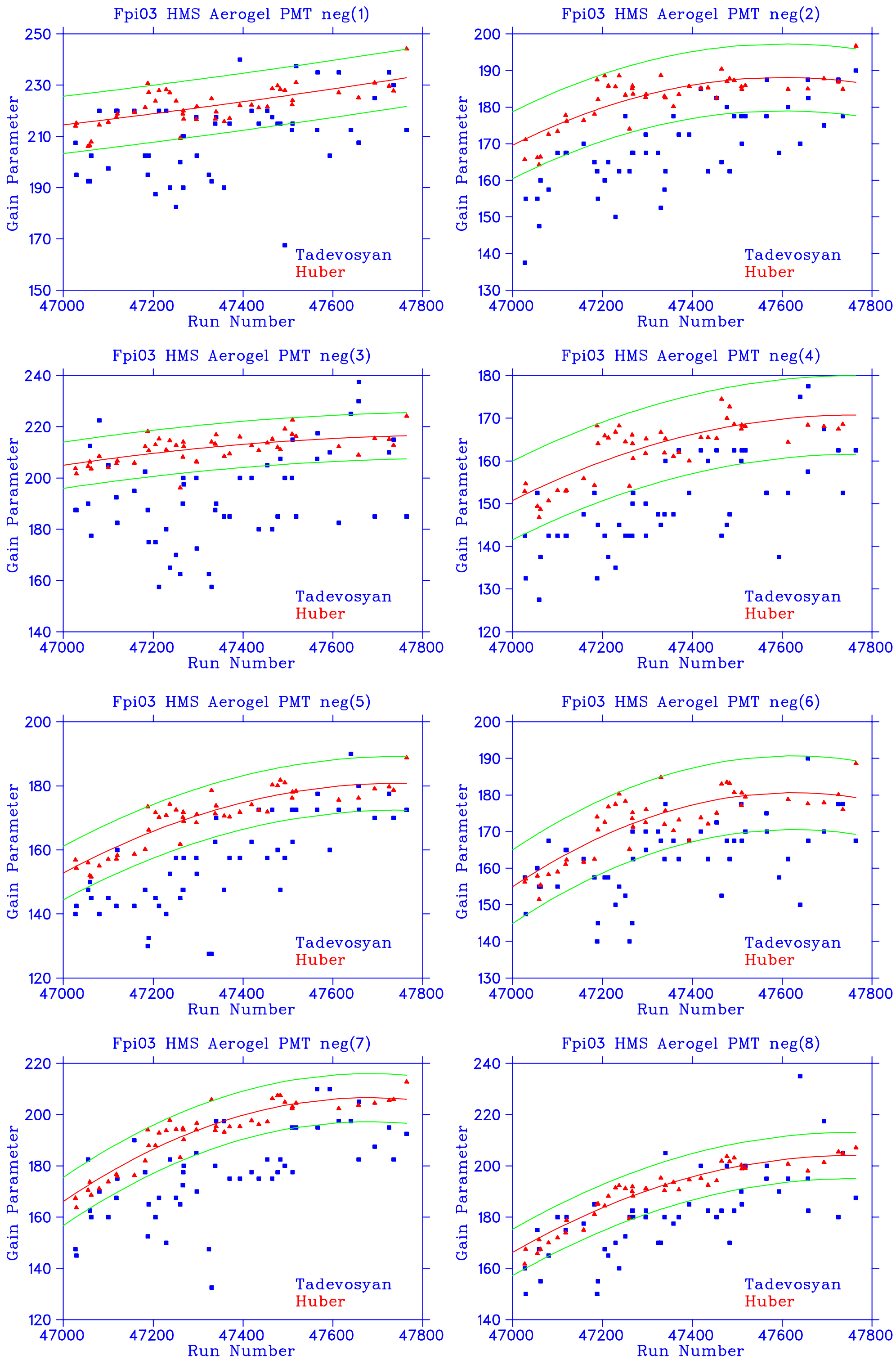

Figure 3: Gain parameters for negative pmts 1-8. The red curve is a quadratic fit to the run dependence to indicate the long-term gain increase. The two green curves indicate the $\pm 2\sigma$ deviation from the red curve.

3 Position Dependence

The position dependence of photoelectron output was investigated using data from runs 47419 and 47435, where the HMS has a central momentum of +3.336 GeV/c. The aerogel focal plane co-ordinates are calculated for a z-value of 69.1 cm. Between 12 and 14 photoelectrons are typically produced (Fig. 4).

The left-right uniformity of the detector response is within 10%, with a greater number of photoelectrons detected when the particles pass near the pmts than when they pass through the middle of the box, as expected. The top-bottom uniformity is within 20%. The top and bottom regions yield fewer photoelectrons because there are no pmts located along the top and bottom edges of the aerogel enclosure. Therefore, for these regions the total solid angle of the pmt photocathodes are lower. At high $Xaer$ (the bottom of the detector with high momentum pions) the response is a bit worse than at low $Xaer$ (the top of the detector with lower momentum pions). This is the opposite of what one might expect from the β dependence of Cerenkov light production, and is not understood.

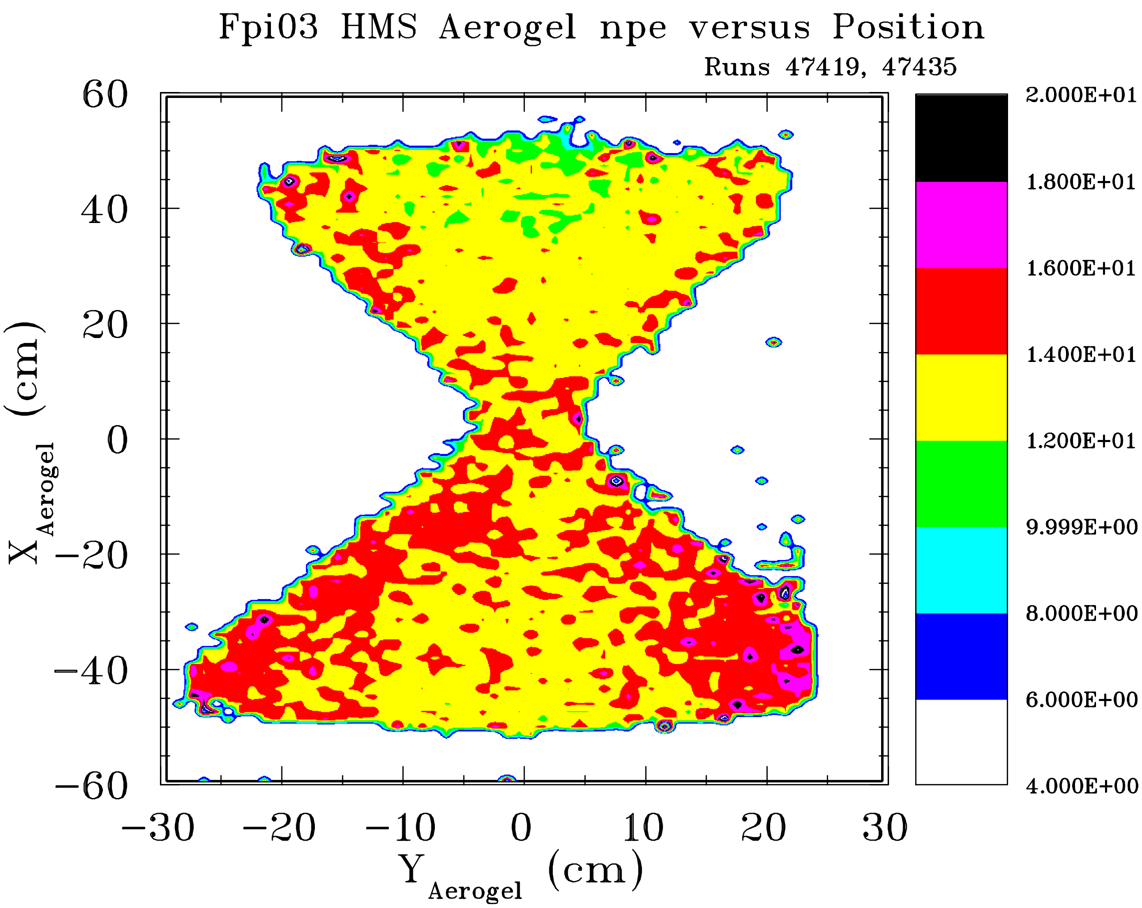

Figure 4: Position dependence of photoelectron response for π^+ with an HMS setting of +3.336 GeV/c. Pion events were selected by requiring npe> 2.5.

4 Velocity Dependence and Recommended Cut

When investigating the dependence of the photoelectron output with the velocity of the incident particle, a minor error was discovered in `h_aero.f`. Formerly, the summed number of photoelectrons was incremented only for those adcs who exceed their pedestal values. Since only pmts whose noise for that event is greater than their statistical means are thus included, this resulted in a skewed npe sum for low velocity events, such as protons below the Cerenkov threshold (Fig. 5a). Using this routine, the Yerevan group found a 'npe floor' of 1.4 p.e. for particles below Cerenkov threshold for the Spring03 data.

The modified routine sums photoelectrons for all pmts, regardless of whether they are above or below their pedestals, so that the noise contribution sums to its average value (i.e. zero, if the calibration is done correctly). The corrected result is much closer to zero (Fig. 5b), as expected. In order to assure that your data replay incorporates this fix, use only Revision 1.4 of `h_aero.f` (dated 2004/02/27), or later.

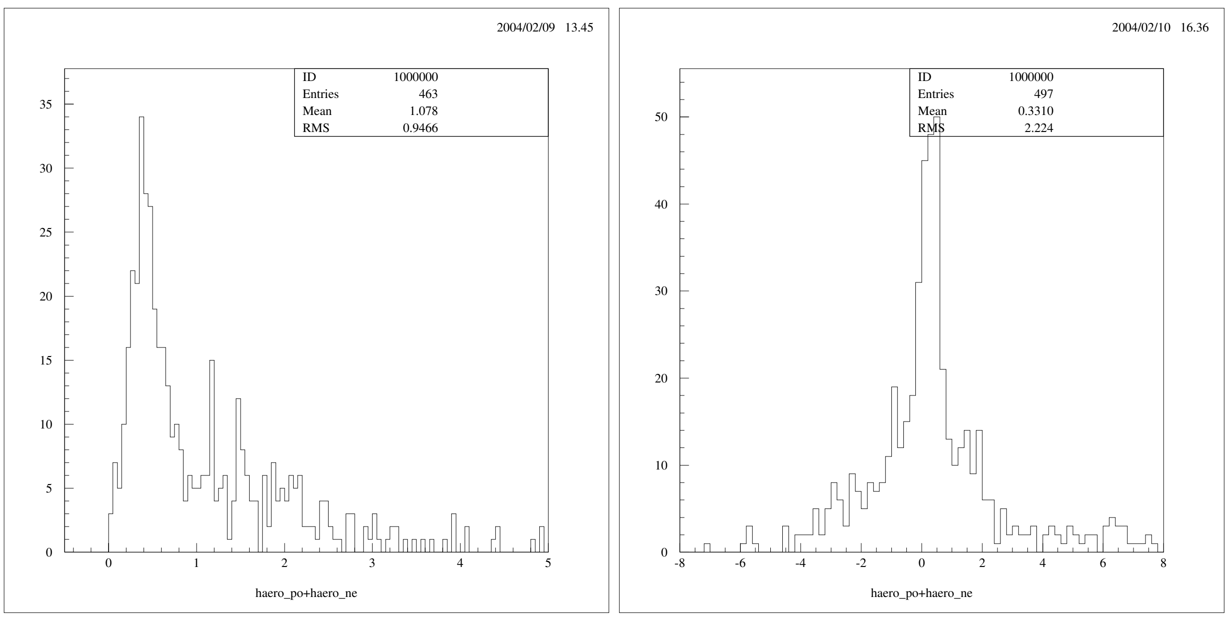

Figure 5: Summed number of photoelectrons for protons below Cerenkov threshold in run 47593. The HMS is set to 2.931 GeV/c, which is 10% below the proton Cerenkov thereshold of 3.278 GeV/c. Cuts have been placed on the coincidence time to select protons and on $hsxfp$ to select the low momentum side of the focal plane. The plot on the left sums pmts who are only above their pedestal value, resulting in an average of 1 photoelectron detected, even when the particle is below Cerenkov threshold. The plot on the right is for the same data, but now sums all pmts without restriction. The corrected result is now consistent with zero photoelectrons detected.

After correcting this minor error, one obtains a mean number of photoelectrons detected of 0.2 for protons below Cerenkov threshold (see Fig. 6). For the highest momentum run in Fpi-2 (+4.335 GeV/c), protons are above the Cerenkov threshold, with a mean of 3.4 photoelectrons obtained. Assuming Poisson statistics centered at 13 p.e., a cut at 3 photoelectrons to eliminate protons should identify pions with an efficiency $> 99.9\%$. In combination with a coincidence time cut, this should effectively eliminate protons.

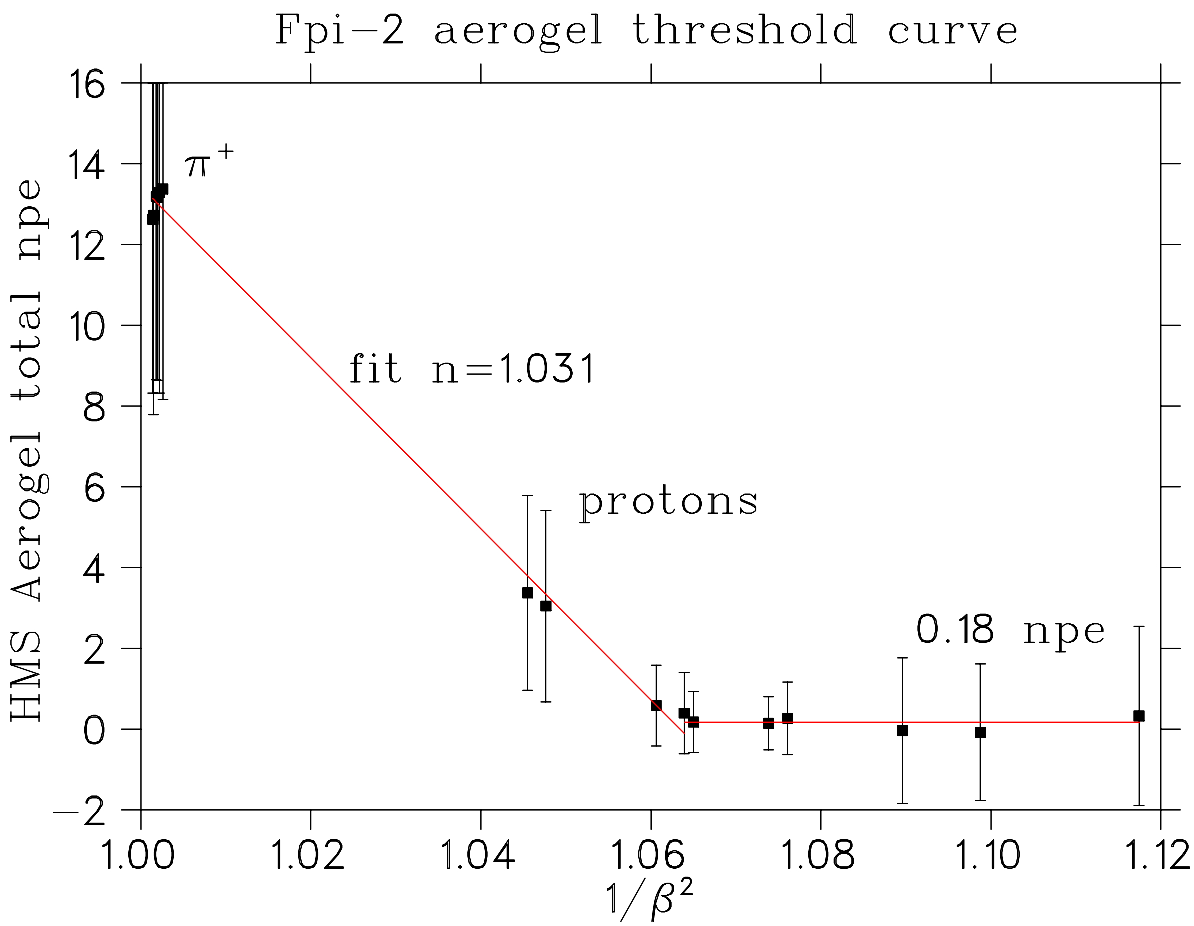

Figure 6: Aerogel threshold curve obtained from Fpi-2 runs. The proton data are from HMS settings of +2.931 to +4.335 GeV/c, separated from pions using the coincidence time. The π^+ data are from HMS settings of +2.931 to +3.412 GeV/c, with $\beta > 0.998$; in this case a second cut was applied to exclude events with npe< 2. The error bars indicate the widths of the summed photoelectron distributions, and the squares indicate the respective means. A flat fit of the $\beta = 0.946$ to 0.964 data gives a mean number of photoelectrons detected below threshold of 0.2. A fit of the $\beta \geq 0.9695$ proton and π^+ data yields a fit index of refraction of $n = 1.0308$.

5 Unresolved Problems

For most events, the tdc information is missing. This is clearly shown in Fig. 7, where the tdc multiplicity is usually only 0 or 1 per detector side, even though an average of 8 pmts actually fire (as determined from adc information). The reason for this discrepancy is that the pmt linear outputs are somewhat attenuated by the time they get to the counting room, and the discriminator levels applied to them (50 mV) are too high. This is not a big problem, but if one wishes to place tdc cuts in the future in order to remove non-time-correlated events, this needs to be fixed.

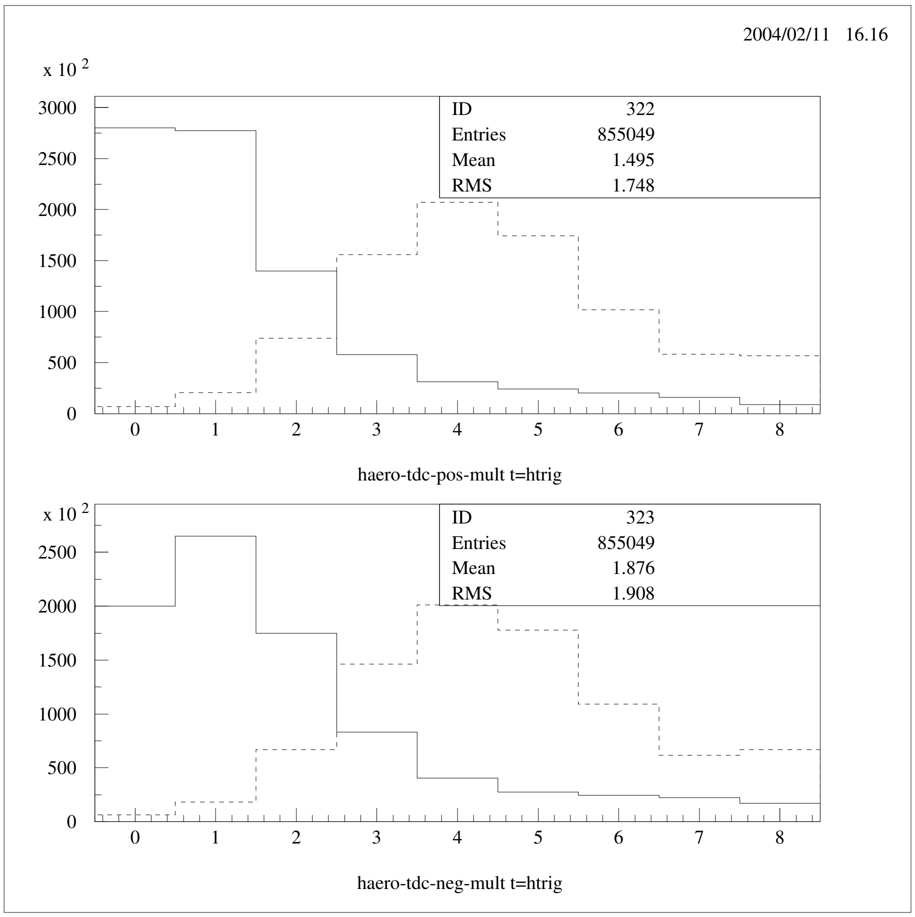

Figure 7: PMT multiplicity calculated for the HMS aerogel detector using tdc information (solid lines) and from adc information (dashed lines). In this case, the adc sum is incremented every time a pmt has > 0.3 pe; the tdc sum is incremented for all pmts less than time-out. In principle, the two curves should agree.